sustainability

MDPI

Article

Historical and Future Changes in Water Temperature in the Pilica River (Central Europe) in Response to Global Warming

Mariusz Ptak [1,*], Teerachai Amnuaylojaroen [2,3] and Mariusz Sojka [4]

[1] Department of Hydrology and Water Management, Adam Mickiewicz University, Krygowskiego 10, 61-680 Poznań, Poland
[2] School of Energy and Environment, University of Phayao, Phayao 56000, Thailand; teerachai4@gmail.com
[3] Atmospheric Pollution and Climate Research Unit, School of Energy and Environment, University of Phayao, Phayao 56000, Thailand
[4] Department of Land Improvement, Environmental Development and Spatial Management, Poznań University of Life Sciences, Piątkowska 94E, 60-649 Poznań, Poland; mariusz.sojka@up.poznan.pl
* Correspondence: marp114@wp.pl

Abstract: This study analyzes changes in the water temperature in the Pilica River (Poland), encompassing both historical data (1958–2023) and projections extending to the year 2100. We use multi-model ensembles (MMEs) with Bayesian Model Averaging (BMA) to integrate various Global Climate Model (GCM) datasets for current and projected climate data. Additionally, a Random Forest (RF) machine learning method is applied to project future water temperatures in the Pilica River. It has been demonstrated that over a period of more than sixty years, the average annual water temperature has increased by nearly 2 °C. Further changes are expected to continue in a similar direction with a gradual rise in this parameter, reaching a temperature increase of 3 °C by the end of the 21st century (SSP585). In the distant future, with average monthly water temperature changes at the Przedbórz station ranging from 0.27 °C to 0.87 °C·decade^{-1} and at the Białobrzegi station from 0.22 °C to 1.06 °C·decade^{-1}. The results of these changes are concerning, especially considering the crucial role of water temperature in shaping seasonality and the dynamics of processes occurring within the river. In the context of the sustainability of the river itself, but also of the entire catchment area, strategies developed by relevant public administration bodies are needed to mitigate the impacts of global warming observed in the thermal regime of the Pilica River.

Keywords: river; water temperature; climate change; sustainability; Poland

Citation: Ptak, M.; Amnuaylojaroen, T.; Sojka, M. Historical and Future Changes in Water Temperature in the Pilica River (Central Europe) in Response to Global Warming. *Sustainability* **2024**, *16*, 10244. https://doi.org/10.3390/su162310244

Academic Editor: Giuseppe Barbaro

Received: 20 September 2024
Revised: 19 November 2024
Accepted: 19 November 2024
Published: 22 November 2024

1. Introduction

Rivers are a vital component of the environment, shaping the Earth's surface, creating biodiversity, and directly influencing human life. The extent of their impact on various subsystems and the potential for human utilization of water resources depend on many interconnected factors related to watershed parameters, as well as the chemical and physical characteristics of the water itself. Among these elements, temperature plays a fundamental role, as its distribution and fluctuations govern cyclical changes in a range of processes [1–5]. Given this context, an approach focusing on understanding the thermal regime of rivers, including its changes—especially long-term changes in light of global warming—is justified. Studies conducted in various parts of the world indicate an increase in water temperature, with the rate of change varying according to the characteristics of individual watersheds.

The results of studies conducted in the Mid-Atlantic Region (USA) showed an increase in first-order streams by 0.32 °C·decade^{-1} and higher-order streams by 0.28 °C·decade^{-1} [6]. In the Yongan River basin (China), the water temperature rose by 0.029 °C

to 046 °C/yr between 1980 and 2012 [7]. In the karst region of Croatia, an analysis of temperature changes in three rivers revealed an increase in the average annual temperature ranging from 0.17 °C to 0.48 °C·decade^{-1} [8]. Since 1946, the Hudson River has warmed by 0.945 °C primarily due to rising air temperatures. Significant seasonal changes have occurred from April to August [9]. The projected average temperature of the Ganges River is expected to increase by 0.58 °C and 0.63 °C for urban and non-urban sections, respectively, by 2025 compared to 2022 [10]. Trends in the annual average water temperatures of the Danube and Sava Rivers from 1956 to 2020 have shown a steady increase, amounting to increases of 0.34 °C and 0.44 °C per decade, respectively [11].

River water temperature depends on numerous variables, including water flow, groundwater inflow, land use, thermal pollution, and air temperature [12–16]. As previously indicated, changes in water temperature reflect climate changes, with air temperature playing a crucial role. An analysis of rivers in Canada confirms that the average air temperature and its trends are the main driving factors behind the average water temperature and its trends [17]. This is further supported by studies in Europe [18], which also highlight the importance of air temperature in influencing changes in water temperature. Moreover, it is important to emphasize the availability and completeness of air temperature measurements, which is particularly crucial in analyses spanning several decades.

In Poland, the analysis of trends in water temperature changes in flowing waters is also a subject of considerable interest, both concerning transit rivers [19] and smaller ones [20]. However, studies addressing future changes in this parameter have not received extensive attention thus far. Piotrowski et al. [21] analyzed two rivers in Poland, indicating that water temperatures will be 2–3.5 °C higher in spring and autumn and below 2 °C higher in summer and winter months. Compared to studies in other countries [22–24], the lack of broader knowledge regarding future changes represents a significant gap for this part of Europe.

Beyond the knowledge related to major rivers significant on the scale of individual continents, it is important to understand the role of river ecosystems in smaller spatial contexts such as regions or watersheds. This creates a solid foundation for effective management, ultimately leading to the maximization of ecosystem benefits for local communities. In this context, having an outline of knowledge regarding future changes is crucial. This study conducts such an analysis for the Pilica River (central Poland), where detailed water temperature observations have been carried out for over six decades, making it one of the longest datasets available in this field. Additionally, it should be emphasized that the Pilica River itself, as well as its watershed, is of interest to various scientific fields [25–28], and current research expands existing knowledge by addressing forecasts of future thermal conditions of the water.

The aim of this article is to determine the historical and future changes in the thermal regime of the Pilica River, referring in detail to the annual and monthly mean temperatures of two hydrological stations—Przedbórz and Białobrzegi.

2. Materials and Methods

2.1. Study Area

The subject of this research is the Pilica River, located in south-central Poland. It is the longest left tributary of the Vistula River, the largest river in Poland (Figure 1). According to Jagiełło [29], the length of the Pilica is 340.5 km, with an average drop of 75 cm/km and a catchment area of 9252 square kilometers, ranking it ninth in Poland in this regard. The land use structure is dominated by fields and meadows (66%), followed by forests (24%) and built-up areas (10%). In terms of flow, the river has a moderately developed nival regime, meaning that spring discharge ranges from 130% to 180% of the annual discharge. Rivers in this group have monthly discharge coefficients (Pardé coefficients) between 1.3 and 1.8 [30,31]. The average flow during the analysis period was 43.9 m^3·s^{-1}. The river serves as a source of drinking water for towns and villages and is

also used for irrigation. Additionally, due to its scenic values, it is a popular destination for tourism and recreation, including activities such as fishing and kayaking.

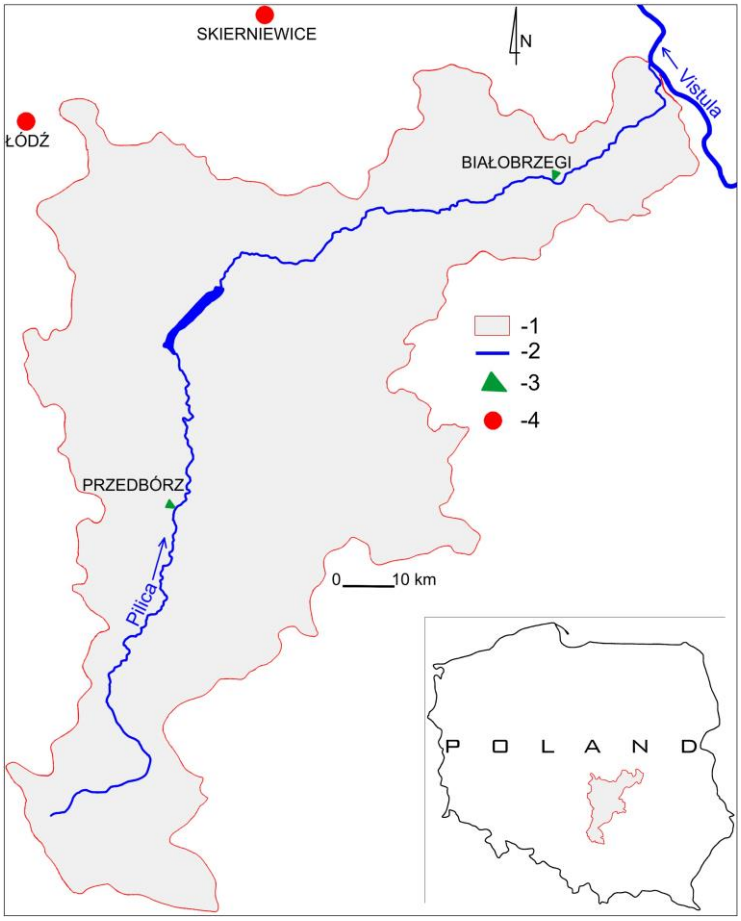

Figure 1. The location of the study area: 1—catchment; 2—water; 3—hydrological stations; 4—meteorological stations.

2.2. Matarials

Water temperature data for the Pilica River were collected at two hydrological stations: Przedbórz (201 km of the river course, 187.2 m above sea level) and Białobrzegi (45.3 km of the river course, 111.9 m above sea level). The dataset covers a total period of 66 years (1958–2023). Water temperature measurements were conducted by the Institute of Meteorology and Water Management-National Research Institute a depth of 0.4 m below the surface, always at the same point near the gauge. Additionally, we utilized air temperature data from two stations (Łódź and Skierniewice), which were also collected by the Institute of Meteorology and Water Management-National Research Institute as part of standard monitoring efforts.

2.3. Methods

We used multi-model ensembles (MMEs) with Bayesian Model Averaging (BMA) to integrate various Global Climate Model (GCM) datasets for current and projected climate data. Additionally, a Random Forest (RF) machine learning method was applied to project future water temperatures in the Pilica River, with MMEs reducing individual model uncertainties. Bias correction was applied to all climate datasets to improve data validity before water temperature prediction. Predictions were made for each location along the river and averaged to represent overall river conditions. To capture gradual temperature trends across historical and future periods, time was incorporated as a continuous variable in both RF and BMA models. This approach reflects the temporal evolution of climate

impacts on water temperature, enabling the models to detect shifts over extended periods as climate effects intensify.

The ensemble comprises nine Global Climate Models (GCMs) obtained from Coupled Model Intercomparison Project Phase 6 (CMIP6), including Norwegian Earth System Model version 2; medium resolution (NorESM2-MM) [32]; Max Planck Institute Earth System Model version 1.2, high resolution (MPI-ESM1-2-HR) [33]; European Consortium Earth System Model version 3 (EC-Earth3) [34]; Alfred Wegener Institute Climate Model version 1.1, medium resolution (AWI-CM-1-1-MR) [35]; Beijing Climate Center Climate System Model version 2, medium resolution (BCC-CSM2-MR) [36]; Meteorological Research Institute Earth System Model version 2.0 (MRI-ESM2-0) [37]; Geophysical Fluid Dynamics Laboratory Earth System Model version 4 (GFDL-ESM4) [38]; Community Earth System Model version 2 with Whole Atmosphere Community Climate Model (CESM2-WACCM) [39]; and Euro-Mediterranean Center on Climate Change Climate Model version 2, strategic research configuration (CMCC-CM2-SR5) [40]. Each model presents its surface temperature projections for the period from 2015 to 2100. The predictions are subsequently modified to achieve a consistent spatial resolution across the group. The regridding process employs linear interpolation to align model outputs with a specified grid of latitude and longitude, facilitating a direct comparison. We utilize a regridding method to interpolate the model data onto a uniform grid.

The regridding process involves calculating an interpolated value for each point on the target grid, defined by coordinates (x_t, y_t), using a source grid with coordinates (x_s, y_s). The interpolated value "V" on the target grid is computed for a variable V defined on the source grid by employing a chosen interpolation method. Bilinear interpolation is a widely utilized method [41] mathematically expressed as follows:

$$V'(x_t, y_t) = \sum_{i=1}^{4} w_i \cdot V(x_s^i \cdot y_s^i)$$

The interpolated value $V'(x_t, y_t)$ at the target grid point is calculated using bilinear interpolation, where w_i are weights based on the distances from each of the four nearest grid points $(x_s^i \cdot y_s^i)$ on the source grid to the target point (x_t, y_t). The value $V(x_s^i \cdot y_s^i)$ represents the data at each of the four grid points, and the weights are determined by linear distances.

The weights in bilinear interpolation are estimaed as follows:

$$w_i = \frac{1}{\Delta x \cdot \Delta y} \cdot (x_{dist}^i \cdot y_{dist}^i)$$

Δx and Δy denote the distances between adjacent points on the source grid. The variables x_{dist}^i and y_{dist}^i denote the horizontal and vertical distances, respectively, between the ith neighboring point and the target grid point.

This study employs Bayesian Model Averaging (BMA) [42] to integrate projections from five global climate models (GCMs). BMA is a statistical framework that facilitates the integration of predictions from multiple models through the application of probability theory. This approach is based on Bayes' theorem, which can be mathematically expressed in the context of model averaging as follows:

$$p(M_i|y) = \frac{p(y|M_i) \cdot p(M_i)}{p(y)}$$

$p(M_i|y)$ denotes the posterior probability of model Mi conditioned on the data y. Likewise, $p(y|M_i)$ represents the probability of the data y given model M_i. $p(M_i)$ denotes the prior probability of model M_i, whereas p(y) signifies the marginal likelihood of the data y and functions as a normalizing constant.

Taking a weighted average of the predictive distributions from each model allows one to calculate the BMA predictive distribution for a new observation ($\tilde{y}$)

$$p(\tilde{y}|y) = \sum_{i=1}^{M} p(\tilde{y}|M_i) \cdot p(M_i|y))$$

$p(\tilde{y}|y)$ is the predictive distribution of $\tilde{y}|$ given model M_i, and $p(M_i|y)$ is the posterior probability of model M_i given the observed data y. This weighted sum allows the BMA framework to combine model predictions, accounting for the relative likelihood of each model.

For a given grid point (x, y) and time (t), the ensemble of climate models offers a combined Bayesian Model Averaging (BMA) forecast of the surface temperature (T).

$$T_{BMA}(x, y, t) = \sum_{i=1}^{M} w_i(x, y, t) \cdot T_i\,(x, y, t)$$

Ti (x,y,t) is the forecast that model i produces, while wi (x,y,t) is the weight that model i is assigned by Bayesian Model Averaging (BMA) at grid point (x,y) and time t. The weight is chosen using the location- and time-specific posterior probability p(M_i|y).

The BMA forecast $T_{BMA}(x, y, t)$ at grid point (x,y) and time t is computed as a weighted sum of the individual forecasts $T_i(x, y, t)$ from each model i. The weights $w_i(x, y, t)$ are determined based on the posterior probabilities of each model at the specified grid point and time.

This study employs a variant of the quantile mapping technique for bias correction, specifically utilizing a linear scaling approach [43]. This method uses a conventional statistical technique to align both the mean and variability of the model outputs with observed data. By adjusting the distribution of projected values to better match historical observations, this approach effectively reduces the inherent variability and systematic biases in GCM outputs. This adjustment enhances the reliability of the model predictions, particularly for extreme climate scenarios, by ensuring that both the central tendency and spread of model projections are consistent with actual climate conditions. The adjustment is predicated on the following formula:

$$Corrected\ model = \mu_{obs} + \left(\frac{\mu_{obs}}{\mu_{gcm}}\right) \times (Model - \mu_{gsm})$$

where μ_{obs} and σ_{obs} are the mean and standard deviation of the observed air temperature for each month, respectively. μ_{gcm} and σ_{gcm} are the mean and standard deviation of the model's (GCM) air temperature data for the corresponding month. Model represents the raw model output for air temperature.

We used a Random Forest (RF) machine learning approach to project future water temperatures in the Pilica River. RF is an ensemble learning method that generates multiple decision trees, each trained on a randomly selected subset of the dataset. By averaging the predictions from these trees, RF reduces overfitting and improves accuracy. The model's ability to handle large, high-dimensional datasets makes it effective for downscaling by capturing spatial patterns and relationships in the data. This robustness allows RF to serve as a viable alternative to more complex climate models. An ensemble of many relatively autonomous models, called trees, operating as a committee, outperforms any one component model; this is the fundamental idea behind this method. The equation represents the Random Forest regression prediction, X = {x_1, x_2, x_3,…, x_n }, with matching labels, Y = {y_1, y_2, y_3, …, y_n }, using training examples.

$$f(x) = \frac{1}{B}\sum_{b=1}^{B} f_b(x)$$

B denotes the total number of trees in the forest, and $f_b(x)$ signify the forecast generated by the bth tree.

Hyperparameter optimization is essential for enhancing climate model downscaling through machine learning. In this study, hyperparameters were tuned using a grid search and k-fold cross-validation to improve model robustness and reduce overfitting. The dataset was split 70–30 for training and testing, with 5-fold cross-validation further validating the results and maximizing data use. The mean squared error (MSE) and Pearson correlation were used as performance metrics as they provide insights into error magnitude and projection alignment. The machine learning models outperformed the original GCM data in downscaling accuracy, with detailed documentation supporting repeatability. Python, version 3.11.9 along with Scikit-learn version 1.3.1 and xarray version 2023.9.0, was used for analysis, ensuring replicability.

For the Random Forest model, optimal settings included 100 trees, a maximum depth of 50, a minimum of 5 data points for splits, and 2 data points per leaf.

To ensure the reliability of our models, we used 5-fold cross-validation, testing each configuration across different data segments. Model performance was assessed using multiple metrics: prediction accuracy (R^2), mean error magnitude (MAE and RMSE), and error dispersion (SD).

$$R^2 = 1 - \left(\frac{\sum(y_i - \hat{y}i_i)^2}{\sum(y_i - \bar{y})^2}\right)$$

$$MAE = \frac{1}{n}(\sum|y_i - \hat{y}_i|$$

$$RMSE = \sqrt{\left[\frac{1}{n}\sum(y_i - \hat{y}_i)^2\right]}$$

where y_i are the observed values, $\hat{y}_i$ are the predicted values, $\bar{y}$ is the mean of the observed values, and n is the number of observations.

The efficacy and generalization ability of the Random Forest model as the training size escalates for both Białobrzegi and Przedbórz are illustrated in Figure 2.

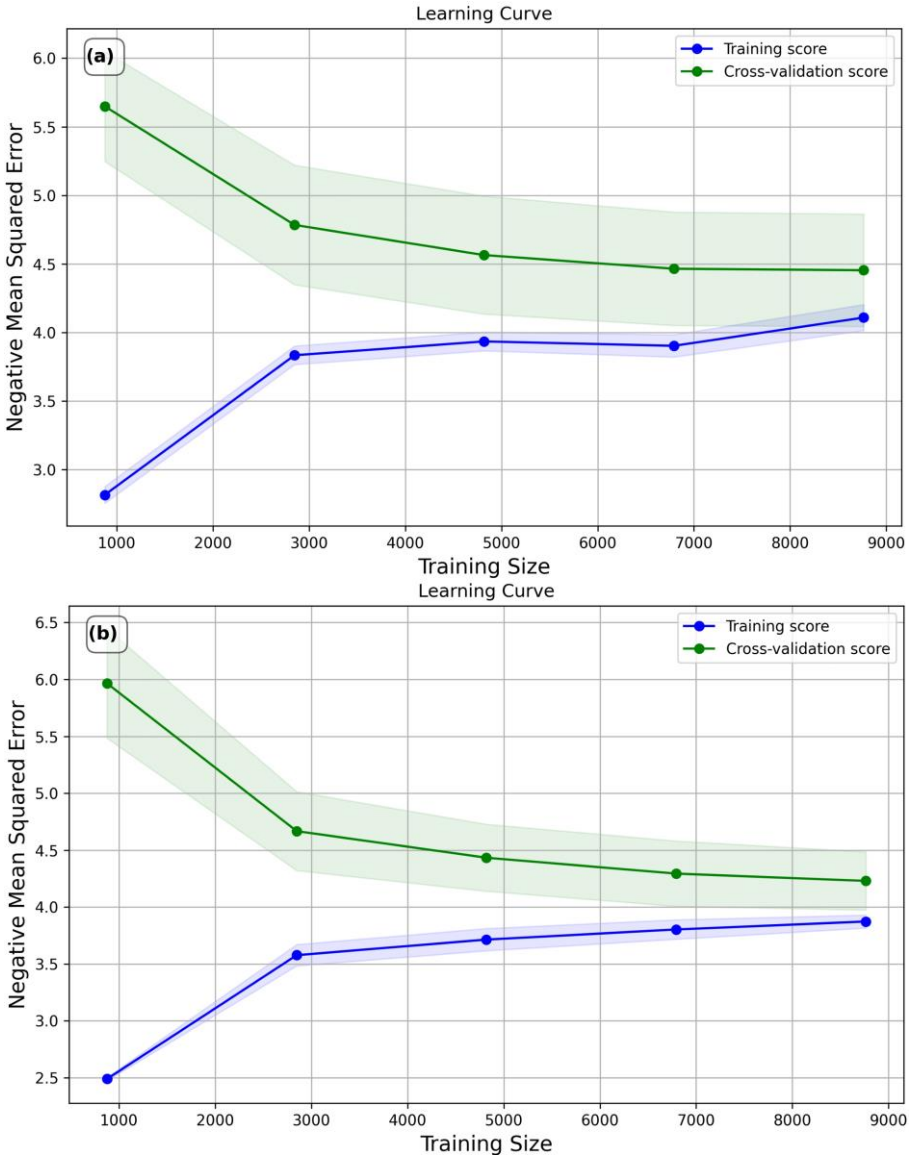

Figure 2. Learning curve for the (**a**) Białobrzegi station; and (**b**) Przedbórz station.

As shown in Figure 2, the training score (blue line) consistently rises in error as the training size increases, stabilizing at a higher level due to added data variability and noise. The cross-validation score (green line) shows an initial high error that decreases and stabilizes with larger training sizes, indicating reduced overfitting and improved generalization. The convergence of training and cross-validation errors suggests that adding data enhances the model's balance between fitting and generalizing.

The shaded regions in Figure 2 represent the standard deviation of errors, which is higher with smaller training sizes and diminishes as the training size grows, indicating improved model stability. Table 1 further supports these results: high mean R^2 values (0.90 for Przedbórz and 0.92 for Białobrzegi) show a strong correlation between the predicted and observed values, while low mean MAE (1.59 °C and 1.60 °C) and mean RMSE (2.06 °C and 2.11 °C) values indicate high prediction accuracy. Additionally, low standard deviations (SD) for R^2, MAE, and RMSE in Table 1 reflect the model's consistent performance across datasets.

Table 1. Performance metrics of machine learning models at Przedbórz and Białobrzegi.

Station	Mean R^2 (-)	SD R^2 (-)	Mean MAE (°C)	SD MAE (°C)	Mean RMSE (°C)	SD RMSE (°C)
Przedbórz	0.90	0.01	1.59	0.05	2.06	0.06
Białobrzegi	0.92	0.01	1.60	0.08	2.11	0.10

Based on the measurement data from the hydrological years 1958–2023 and the results obtained using the Random Forest method for the years 2024–2100 under scenarios SSP245 and SSP585, the average monthly and annual water temperatures at the hydrological stations of Przedbórz and Białobrzegi were calculated. In the first stage of the analysis, the non-parametric Pettitt test was applied to identify change points in the air temperature time series from the meteorological stations in Łódź and Skierniewice for the years 1958–2023. The Pettitt test allows for the detection of single change points in mean yearly air temperature time series [44]. This analysis revealed that the change point in both air temperature series occurred in the year 1988, considering the average annual values. The data from scenarios SSP245 and SSP585 were analyzed for near-future (2024–2050), mid-range (2051–2075), and far-future periods (2076–2100). Additionally, the long-term changes in water temperature in the Pilica River at the hydrological stations of Przedbórz and Białobrzegi were examined for the 1958–2100 and 2024–2100 periods under scenarios SSP245 and SSP585. To determine the trends and magnitudes of changes in average annual and monthly water temperatures at the Przedbórz and Białobrzegi stations, non-parametric Mann–Kendall [45] and Sen's [46] slope estimation methods were utilized. The test assumes two hypotheses: the null hypothesis (H0) states that the data do not exhibit a trend, while the alternative hypothesis (HA) suggests that a trend exists. The magnitude of changes in air and water temperatures was determined using the non-parametric Sen's test, which is not sensitive to the presence of outliers. During the data analysis, a pre-whitening procedure was applied to remove autocorrelation from the data series [47]. The Mann–Kendall and Sen tests were performed using the modified "mk" package developed by Patakamuri and O'Brien [48]. The change points were detected using the "trend" package developed by Pohlert [49].

3. Results

3.1. Model Performance

Figure 3 illustrates the relationship between the observed and bias-corrected model air temperature at two locations: Przedbórz and Białobrzegi. The scatter plots reveal strong positive correlations between the observed and corrected temperatures at both sites, demonstrating the effectiveness of the bias correction method in aligning the model outputs with the observational data.

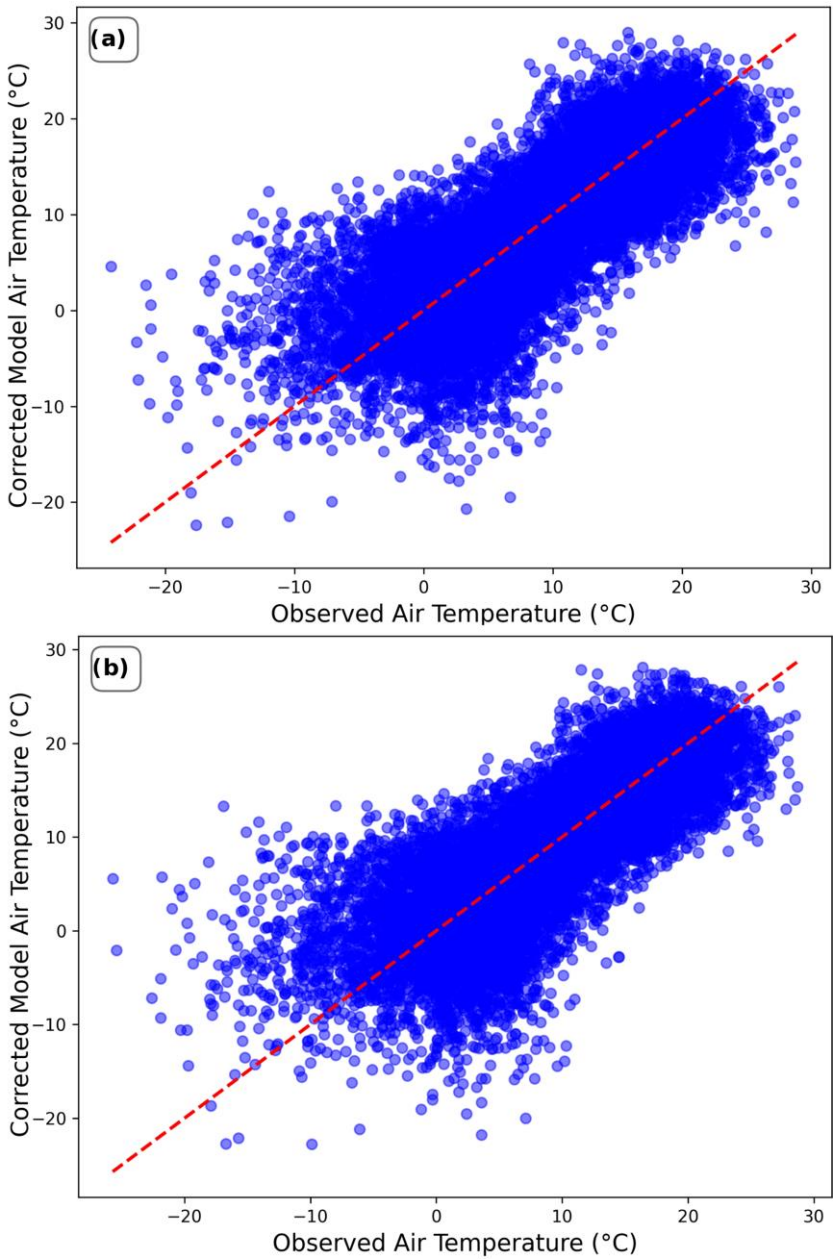

Figure 3. Scatter plot between observed and correct air temperatures at (**a**) Przedbórz station and (**b**) Białobrzegi station.

At the Przedbórz station (Figure 3a), the result shows that the corrected temperatures closely approximate the observed values. Nonetheless, a discernible deviation exists around the line, especially at high air temperatures, where the model tends to marginally overestimate or underestimate air temperatures. This distribution indicates that, notwithstanding the general enhancement in accuracy, some residual errors persist due to model constraints or data inconsistencies. Conversely, the plot for the Białobrzegi station (Figure 3b) exhibits a comparably robust positive correlation, indicating an improved overall alignment between the corrected air model temperature and the observations. Although some discrepancies persist at extreme temperatures, the bias correction seems more efficacious at Białobrzegi, exhibiting diminished variances across a wider spectrum of values. The bias correction method effectively reduces discrepancies between the observed and model temperatures at both stations. The closer aggregation of data points around the optimal line for Białobrzegi indicates a slightly better model performance or reduced variability in observations at this station relative to Przedbórz.

Although the correction enhanced the concordance between the observed and modeled temperatures, some variability persists, particularly at the extremes of the temperature spectrum. Additional enhancements to the model and rectification techniques may aid in reducing these residual errors.

Accurate air temperature predictions are essential for reliable water temperature modeling because air temperature directly influences the thermal dynamics of river systems. Figure 3 demonstrates that the bias correction effectively aligns the modeled air temperatures with the observed values at the Przedbórz and Białobrzegi stations. This correction step is crucial as it reduces errors in the air temperature data, which, in turn, improves the accuracy of the water temperature predictions shown in Figure 4. By ensuring that the input air temperature data are accurate, the model can more precisely predict water temperatures, thereby enhancing the reliability of the results. The strong correlation observed in Figure 3 provides a foundation for the high accuracy in water temperature predictions presented in Figure 4, underscoring the interconnected nature of accurate input data and reliable model outcomes.

The scatter plots (Figure 4) depict the correlation between the observed and predicted water temperatures. Both plots exhibit a robust positive correlation between the observed and predicted temperatures, suggesting that the model effectively captures the fluctuations in water temperature at both sites.

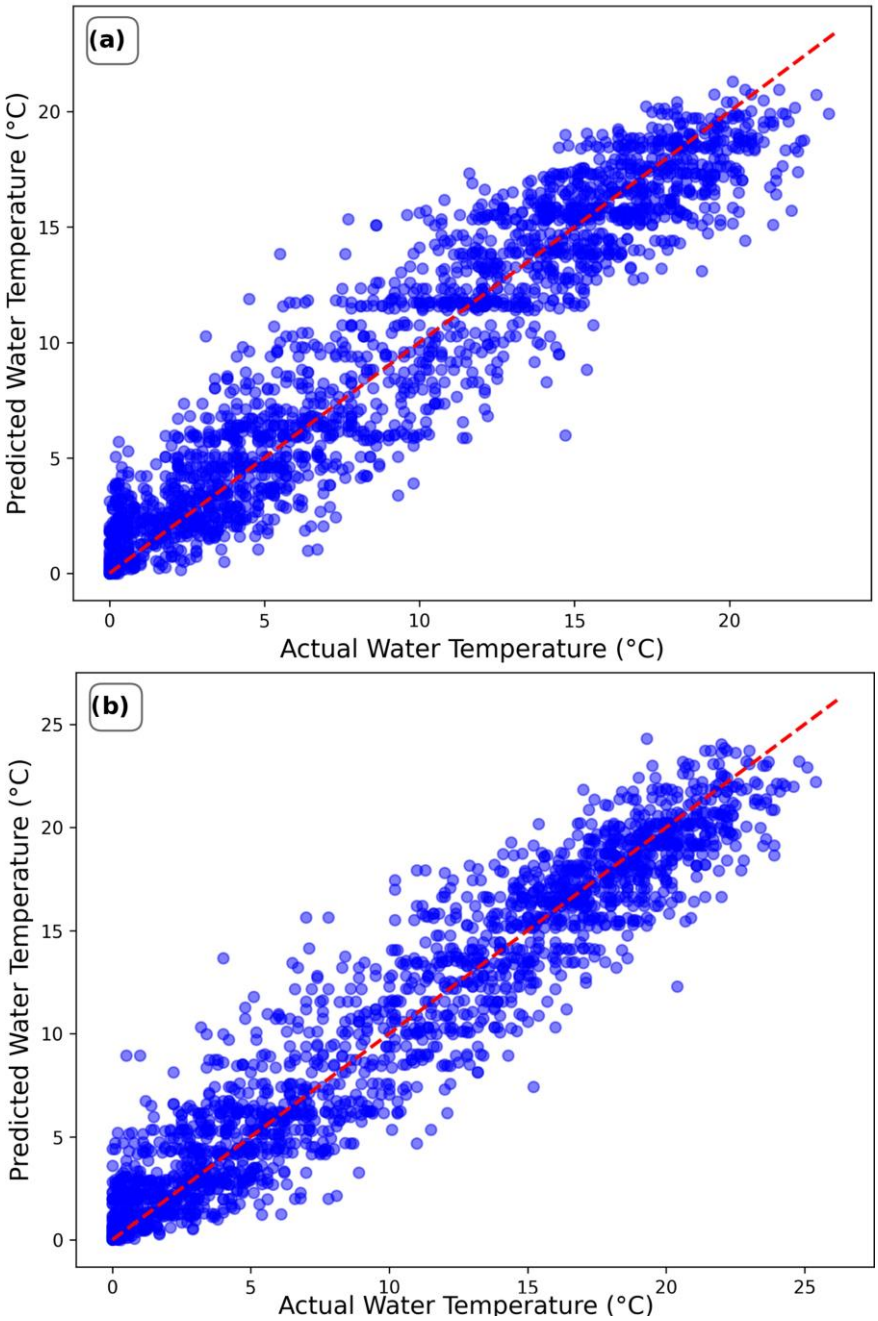

Figure 4. Scatter plot between observed and model water temperature at (**a**) Przedbórz station and (**b**) Białobrzegi station.

Nonetheless, significant deviations along the line, particularly at higher temperature ranges, suggest minor inconsistencies where the model tends to marginally overestimate or underestimate the temperatures (Figure 4a). This spread indicates that although the model adequately reflects the general trend in water temperature, there are regions where its predictions lack precision. Likewise, for the Białobrzegi station, Figure 4b illustrates a robust correlation between the observed and predicted water temperatures. The clustering at Białobrzegi is more compact than that at Przedbórz, indicating marginally superior model performance with reduced deviations from the optimal relationship. Nonetheless, variability persists at the upper limit of the temperature spectrum, suggesting slight overestimation or underestimation by the model under extreme conditions.

Table 2 presents the performance metrics, comparing the simulated water and air temperatures at the Przedbórz and Białobrzegi stations. These metrics include the coefficient of determination (R^2), Mean Absolute Error (MAE), and Root Mean Squared Error (RMSE), providing insights into the model's accuracy and reliability. In Figure 3, the strong positive correlation between the observed and bias-corrected air temperatures demonstrates the effectiveness of the bias correction, with R^2 values of 0.78 and 0.77 for Przedbórz and Białobrzegi, respectively. Although minor residual errors remain, particularly at extreme values, the corrected model outputs closely align with the observational data. Figure 4 shows the correlation between the observed and predicted water temperatures, with higher R^2 values of 0.90 and 0.92 at Przedbórz and Białobrzegi, respectively, indicating that the model captures water temperature variations effectively. The MAE and RMSE values for water temperature are notably lower than those for air temperature, underscoring the model's greater accuracy in predicting water temperatures. Overall, these performance metrics in Table 2 underscore the model's efficacy in estimating water temperatures while identifying opportunities for refinement in air temperature predictions, particularly at the extremes.

Table 2. Performance metrics of modeled water temperature and air temperature at Przedbórz and Białobrzegi.

Station	R^2 Temperature		MAE Temperature (°C)		RMSE Temperature (°C)	
	Water	Air	Water	Air	Water	Air
Przedbórz	0.90	0.78	1.59	4.39	4.19	5.70
Białobrzegi	0.92	0.77	1.58	5.68	4.40	5.68

3.2. Temperature Trend Analysis

The analysis of trends in average annual water temperature for the historical period revealed that at the Przedbórz hydrological station, there was a temperature decrease of -0.25 °C·decade^{-1} from 1958 to 1987 (Table 3). In contrast, during the same period, no statistically significant changes in water temperature were observed at the second station.

Table 3. Changes in mean annual water temperature in Pilica River (Przedbórz and Białobrzegi stations).

Period	Przedbórz				Białobrzegi			
	S	z-Value	*p*-Value	Sen Slope Value (°C Decade^{-1})	S	z-Value	*p*-Value	Sen Slope Value (°C Decade^{-1})
1958–1987	−118	−2.19	0.028	−0.25	−42	−0.77	0.442	−0.11
1988–2023	275	3.89	0.000	0.43	341	4.83	0.000	0.51
2024–2050 [a]	200	4.39	0.000	0.22	194	4.26	0.000	0.25
2051–2075 [a]	38	0.92	0.359	0.05	66	1.61	0.107	0.11
2076–2100 [a]	53	1.29	0.197	0.06	55	1.34	0.180	0.07
2024–2100 [a]	2024	9.07	0.000	0.14	1984	8.89	0.000	0.15
2024–2050 [b]	193	4.23	0.000	0.33	181	3.97	0.000	0.34
2051–2075 [b]	160	3.95	0.000	0.33	180	4.44	0.000	0.37
2076–2100 [b]	206	5.08	0.000	0.44	205	5.06	0.000	0.49
2024–2100 [b]	2500	11.21	0.000	0.41	2510	11.25	0.000	0.45
1958–2100 [a]	7851	13.85	0.000	0.21	6991	12.33	0.000	0.16
1958–2100 [b]	8471	14.94	0.000	0.35	8546	15.07	0.000	0.38

[a] SSP245; [b] SSP585.

In the period from 1988 to 2023, both hydrological stations showed a significant increase in water temperature. The rate of warming was 0.43 °C at the Przedbórz station and 0.51 °C ·decade^{-1} at the Białobrzegi station. According to the SSP245 scenario, from 2024 to 2100, the water temperature in the Pilica River is expected to continue rising at

rates of 0.14 °C and 0.15 °C ·decade-, respectively. In contrast, under the SSP585 scenario, the rates will be 0.41 °C and 0.45 °C ·decade^{-1}. These differing rates underscore the impact of scenario assumptions on projected warming. When analyzing changes in water temperatures for the near, medium, and distant future under scenario SSP245, a significant increase is anticipated only in the near future, with rates of 0.22 °C and 0.25 °C·decade^{-1} at the Przedbórz and Białobrzegi stations, respectively. In the medium and distant future under scenario SSP245, no significant changes in water temperature in the Pilica River are expected. However, considering scenario SSP85 for the near, medium, and distant future, significant increases in water temperature will occur. The lowest increments are expected in the near future at 0.33 °C and 0.34 °C·decade^{-1}, while the highest increases will be in the distant future at rates of 0.44 °C and 0.49 °C/decade, respectively, at the Przedbórz and Białobrzegi stations. Throughout the entire period from 1958 to 2100, the changes in water temperature at the Przedbórz station are slightly lower than those at the Białobrzegi station. According to scenario SSP245, the average increase in water temperature from 1958 to 2100 at the Przedbórz and Białobrzegi stations will be 0.21 °C and 0.16 °C·decade^{-1}, respectively, while under scenario SSP585, the increases will be 0.35 °C and 0.38 °C·decade^{-1}. These results highlight the contrasting temperature trajectories under different climate scenarios as well as the greater sensitivity of the Białobrzegi station to climate impacts. The results of the trend analysis are graphically presented in Figure 5.

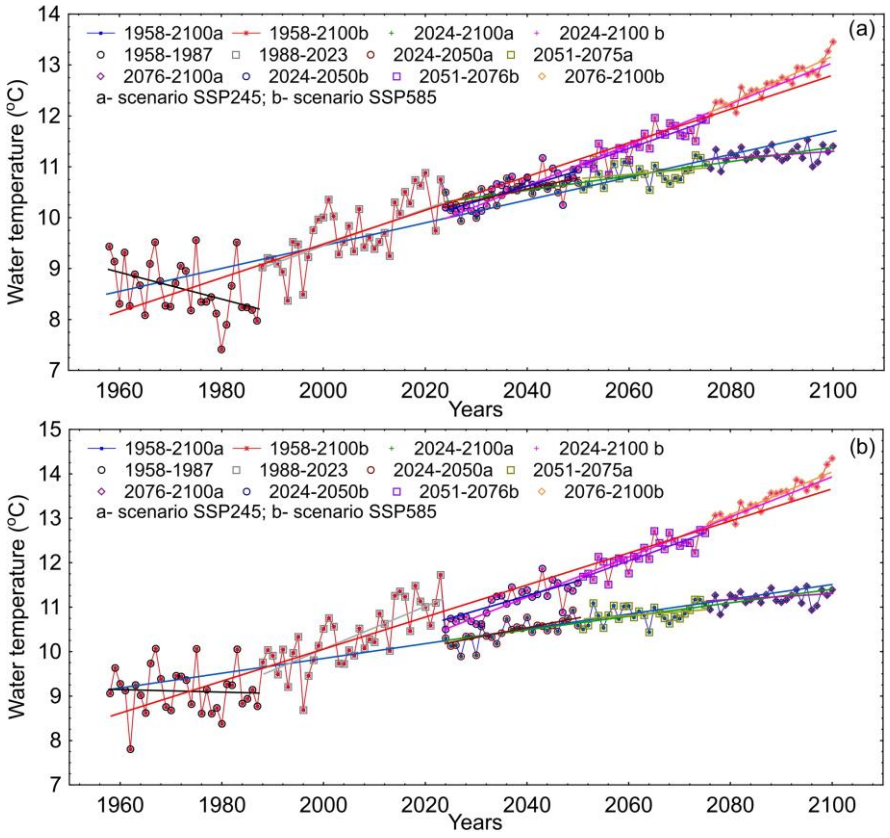

Figure 5. Changes in mean annual water temperature in Pilica River: (**a**) Przedbórz and (**b**) Białobrzegi.

The results of the changes in average monthly water temperature in the Pilica River are presented in Tables S1 and S2. In the period from 1958 to 1987, only in November at the Przedbórz hydrological station were temperatures significantly lower (−0.83 °C/decade), while at the Białobrzegi station, significant decreases were observed in April and June (−0.56–−0.62 °C/decade). In the subsequent period from 1988 to 2023, significant

increases in water temperature were recorded in seven months (from June to December) at both the Przedbórz and Białobrzegi stations, with increases ranging from 0.52 °C to 0.98 °C at Przedbórz and from 0.47 °C to 0.97 °C/decade at Białobrzegi. According to scenario SSP245, only in the near future (2024–2050) is it expected that further increases in water temperature in the Pilica River will occur from June to December at the Przedbórz station and from June to October and December at the Białobrzegi station. In both the near and distant future, changes in the average monthly water temperature will only be observed in isolated months. Under scenario SSP585, changes in the average monthly water temperature will occur more frequently, spanning from 6 to 10 months at both hydrological stations. The most significant changes will be observed in the distant future, with average monthly water temperature changes at the Przedbórz station ranging from 0.27 °C to 0.87 °C/decade and at the Białobrzegi station from 0.22 °C to 1.06 °C/decade.

4. Discussion

4.1. Historical and Future Temperature Changes

Knowledge regarding thermal changes in rivers is an increasingly common topic in hydrology, justified by the fundamental significance of this parameter for the functioning of these ecosystems [50]. Moreover, the close relationship between water temperature and air temperature has led to a widespread transformation observed as river warming, indicating a need for a new perspective on previously known processes. Such observations have also been noted for the river analyzed in this study, where historical records of water temperature indicate an upward trend. Over a period of more than sixty years, the average water temperature in the Pilica River has increased by approximately 0.32 °C/decade, with the respective values for the two stations being 0.29 °C/decade (Przedbórz) and 0.35 °C/decade (Białobrzegi). This finding, showing a rise in water temperature, aligns with other studies on similar topics. As indicated in the introduction, the scale of this process varies, with the climate zone generally being a crucial factor, followed by local conditions in a given watershed and the period of analysis. The water temperature of the Drava River increased by 1.4 °C from 1969 to 2010 [51]. Average stream temperatures in Southern England rose by 2.1–2.9 °C in winter and by 1.1–1.5 °C in summer between 1980 and 2006 [52]. Over the past six decades, the average annual water temperature of the Biebrza River has warmed at a rate of 0.28 °C per decade [53]. Eighteen glacial and non-glacial streams in the European Alps experienced summer warming at an average rate of 2.5 °C per decade [54]. In southeastern Australia, stream temperature trends indicate an increase in the average annual temperature of 1 °C between 1992 and 2021 [55]. Particularly interesting are the results obtained later in this study, which indicate that the temperature increase will continue, reaching an average annual increase of 1.0 °C (SSP245) by the end of the 21st century and 3.0 °C according to different scenarios (SSP285). As mentioned earlier, the response of the Pilica River to ongoing global warming does not differ from that of other rivers, where further increases in water temperature are also predicted [56–58]. While this study utilizes CMIP6-based GCMs integrated through Bayesian Model Averaging (BMA) to improve projection reliability, it is important to acknowledge the limitations of using global climate models alone to capture localized climate dynamics accurately. GCMs are designed to provide insights on large-scale climate patterns and trends, yet their relatively coarse resolution may not fully capture specific regional characteristics, such as localized temperature variations or microclimatic effects that can impact river systems like the Pilica River basin.

4.2. Management Implications and Mitigation Strategies

Currently observed and simulated future changes in the thermal regime of the Pilica River should be regarded as unfavorable. The permanently rising water temperature will determine a range of transformations that, due to the complexity of these interactions, are difficult to predict. One of the key factors, both ecologically and economically, is water quality. According to the classification of uniform parts of surface water [59], the analyzed

monitoring stations are located in the following sections: Pilica from Zwlecz to the Sulejów reservoir and Pilica from the Sulejów reservoir to the river mouth. For both of these segments, the water status has been classified as poor, with the main sources of chemical pressure being urban development, transportation, agriculture, tourism, and forestry. Moreover, both sections of the river are at risk of eutrophication [60,61]. The increase in water temperature, driven by climate change, local human activities, and hydrology, has significant potential to exacerbate river water quality degradation and coastal water eutrophication in summer [7]. If the current rate of stream temperature rise continues, it could have a substantial impact on eutrophication and ecosystem processes [62]. As can be seen, the issue of maintaining appropriate parameters is complex, and one of the fundamental elements affecting water quality and its self-purification capabilities is oxygen [63]. The amount of dissolved oxygen in the water is closely related to its temperature, with increases in temperature leading to a decrease in oxygen levels or even total depletion. Based on data from over five hundred rivers in the USA, it has been established that temperature primarily drives the daily dynamics of dissolved oxygen, and its decline in warmer rivers has significant implications for these ecosystems in the future [64].

From a hydrobiological perspective, the Pilica River has seen a noticeable increase in the stability of many rheophilic fish species, which are associated with high environmental requirements, particularly concerning oxygen levels [65]. Over multiple decades, this change has been linked to a reduction in pollutants entering the Pilica [65]. However, the current and future rise in water temperature poses new threats in the form of decreased levels of dissolved oxygen in the water. Previous studies in the middle Vistula basin have shown that the intense development of planktonic algae occurs in lowland river sections, including the Pilica [66]. This phenomenon is attributed to the characteristics of the river, which is shallow, flows slowly, and has a low volume of flow. Therefore, it can be inferred that plankton will respond to the continuous increase in water temperature, leading to changes in the structure of the trophic network. For example, the seasonal succession of plankton communities in the Nakdong River was associated with changes in water temperature, showing significant correlations with the abundance of eight major dominant species [67]. High temperatures will increase phytoplankton abundance and chlorophyll-a content within it [68]. In the case of the Ba Lai River, a significant negative correlation was found between water temperature and the biomass of phytoplankton and diatoms [69].

In the context of the sustainability of the river itself, but also of the entire catchment area, the current and projected future situations present significant challenges for water resource management authorities. Proper river management should be a key component of climate change adaptation and mitigation efforts [70]. An important factor in limiting the rise in water temperature is the presence of shaded areas along riverbanks [71,72]. For instance, studies conducted in western Poland [73] have shown that a comparison of two rivers revealed noticeably lower water temperatures in the watershed with a higher percentage of forest cover (the temperature during the growing season was, on average, 2.6 °C lower). The above findings suggest that the development and maintenance of riparian buffer zones, along with the strategic planting of native tree species along the banks, could be an effective management strategy for the river in question. Implementing such measures would require extensive interdisciplinary analyses, encompassing issues related to hydrology, hydrobiology, ecology, as well as administrative and legal matters.

5. Conclusions

Rivers are particularly sensitive to the impacts of climate change, with noticeable effects on their thermal regimes. The increase in water temperature has been well documented for major river systems across continents, illustrating the overall trends and scales of these transformations. However, it is equally important to gain insights into smaller rivers that play a crucial role in the functioning of specific regions. This study

analyzed changes in the water temperature of the Pilica River based on two monitoring stations that have some of the longest observation records in the country. The findings indicate that, over more than sixty years, the average annual water temperature has increased by nearly 2 °C. A shift in the thermal regime of the Pilica River was identified, with only an upward trend observed in this characteristic after 1988. Projections through the end of the 21st century indicate further increases, with the extreme scenario predicting a rise of up to 3 °C. In the distant future, simulated increases in average monthly water temperatures are expected to range from 0.27 to 0.87 °C per decade at the Przedbórz station and from 0.22 to 1.06 °C per decade at the Białobrzegi station. Given the fundamental importance of temperature for various processes occurring in river ecosystems, these changes should be regarded as particularly detrimental. Future simulations for the Pilica River cover the next seven decades, highlighting the urgent need to develop strategies that could mitigate the effects of global warming, which would be linked to the concept of sustainability.

Supplementary Materials: The following supporting information can be downloaded at: https://www.mdpi.com/article/10.3390/su162310244/s1, Table S1: Changes in average monthly water temperatures of the Pilica River (Przedbórz station); Table S2: Changes in average monthly water temperatures of the Pilica River (Białobrzegi station).

Author Contributions: Conceptualization, M.P.; methodology, M.P., T.A. and M.S.; software, T.A. and M.S; validation, T.A. and M.S.; formal analysis, M.P., T.A. and M.S.; investigation, M.P., T.A. and M.S.; re-sources, M.P. and T.A.; data curation, M.P., T.A. and M.S; writing—original draft preparation, M.P., T.A. and M.S.; writing—review and editing, M.P., T.A. and M.S.; visualization, M.P., T.A. and M.S.; supervision, M.P.; project administration, M.P.; funding acquisition, M.P. All authors have read and agreed to the published version of the manuscript.

Funding: This research received no external funding.

Institutional Review Board Statement: Not applicable.

Informed Consent Statement: Not applicable.

Data Availability Statement: https://danepubliczne.imgw.pl/ (accessed on 10 September 2024).

Acknowledgments: The authors acknowledge the Institute of Meteorology and Water Management–National Research Institute in Poland for providing the data used in this study.

Conflicts of Interest: The authors declare no conflicts of interest.

References

1. Stagliano, D.M. Western pearlshell (*Margaritifera falcata*) extirpation in the Smith River, Montana, with a possible link to warming water temperatures. *West. N. Am. Nat.* **2023**, *83*, 254–263.
2. Jaffe, S.; Qian, S.S.; Mayer, C.M.; Kocovsky, P.M.; Gouveia, A. Assessing the probability of grass carp (*Ctenopharyngodon idella*) spawning in the Sandusky River using discharge and water temperature. *J. Great Lakes Res.* **2024**, *50*, 102303.
3. Ducharne, A. Importance of stream temperature to climate change impact on water quality. *Hydrol. Earth Syst. Sci.* **2008**, *12*, 797–810.
4. Gervasio, M.P.; Soana, E.; Granata, T.; Colombo, D.; Castaldelli, G. Department of Environment An unexpected negative feedback between climate change and eutrophication: Higher temperatures increase denitrification and buffer nitrogen loads in the Po River (Northern Italy). *Environ. Res. Lett.* **2022**, *17*, 084031.
5. Rankinen, K.; Cano Bernal, J.E.; Holmberg, M.; Vuorio, K.; Granlund, K. Identifying multiple stressors that influence eutrophication in a Finnish agricultural river. *Sci. Total Environ.* **2019**, *658*, 1278–1292.
6. Yao, Y.; Tian, H.; Kalin, L.; Pan, S.; Friedrichs, M.A.M.; Wang, J.; Li, Y. Contrasting stream water temperature responses to global change in the Mid-Atlantic Region of the United States: A process-based modeling study. *J. Hydrol.* **2021**, *601*, 126633.
7. Chen, D.; Hu, M.; Guo, Y.; Dahlgren, R.A. Changes in river water temperature between 1980 and 2012 in Yongan watershed, eastern China: Magnitude, drivers and models. *J. Hydrol.* **2016**, *533*, 191–199.
8. Žganec, K. The effects of water diversion and climate change on hydrological alteration and temperature regime of karst rivers in central Croatia. *Environ. Monit. Assess.* **2012**, *184*, 5705–5723.
9. Seekall, D.A.; Pace, M.L. Climate change drives warming in the Hudson River Estuary, New York (USA). *J. Environ. Monit.* **2011**, *13*, 2321–2327.

10. Das, N.; Sagar, A.; Bhattacharjee, R.; Agnihotri, A.K.; Ohri, A.; Gaur, S. Time series forecasting of temperature and turbidity due to global warming in river ganga at and around Varanasi, India. *Environ. Monit. Assess*. **2022**, *194*, 617.
11. Bonacci, O.; Žaknić-Ćatović, A.; Roje-Bonacci, T.; Prohaska, S.; Bonacci, D.; Ćatović, S. Air and Water Temperature Trend Analysis at the Confluence of the Sava and Danube Rivers in Belgrade, Serbia. *Pure Appl. Geophys.* **2024**, *181*, 2895–2912.
12. LeBlanc, R.T.; Brown, R.D.; FitzGibbon, J.E. Modeling the effects of land use change on the water temperature in unregulated urban streams. *J. Environ. Manag*. **1997**, *49*, 445–469.
13. Moatar, F.; Gailhard, J. Water temperature behaviour in the river Loire since 1976 and 1881. *Comptes Rendus Geosci*. **2006**, *338*, 319–328.
14. Nichols, A.J.; Willis, A.D.; Jeffres, C.A.; Deas, M.L. Water temperature patterns below large groundwater springs: Management implications for Coho Salmon in the Shasta River, California. *River Res. Appl*. **2014**, *30*, 442–455.
15. Abdi, R.; Endreny, T. A River Temperature Model to Assist Managers in Identifying Thermal Pollution Causes and Solutions. *Water* **2019**, *11*, 1060.
16. Nowak, B.; Ptak, M.; Stanek, P. Influence of a lake on river water thermal regime: A case study of Lake Sławianowskie and the Kocunia River (Pomeranian Lakeland, Northern Poland). *Meteorol. Hydrol. Water Manag.* **2020**, *8*, 78–83.
17. Shrestha, R.R.; Pesklevits, J.C.; Bonsal, B.R.; Brannen, R.; Guo, T.; Hoffman, S. Climate Research Division, Rising summer river water temperature across Canada: Spatial patterns and hydroclimatic controls. *Environ. Res. Lett.* **2024**, *19*, 044058.
18. Heddam, S.; Kim, S.; Mehr, A.D.; Zounemat-Kermani, M.; Ptak, M.; Elbeltagi, A.; Malik, A.; Tikhamarine, Y. Bat Algorithm Optimized Extreme Learning Machine (Bat-ELM): A novel Approach for Daily River Water Temperature Modelling. *Geogr. J.* **2023**, *189*, 78–89.
19. Ptak, M.; Sojka, M.; Graf, R.; Choiński, A.; Zhu, S.; Nowak, B. Warming Vistula River–the effects of climate and local conditions on water temperature in one of the largest rivers in Europe. *J. Hydrol. Hydromech.* **2022**, *70*, 1–11.
20. Ptak, M. Long-term temperature fluctuations in rivers of the Fore-Sudetic region in Poland. *Geografie* **2018**, *123*, 279–294.
21. Piotrowski, A.P.; Osuch, M.; Napiorkowski, J.J. Influence of the choice of stream temperature model on the projections of water temperature in rivers. *J. Hydrol.* **2021**, *601*, 126629.
22. Pilgrim, J.M.; Fang, X.; Stefan, H.G. Stream temperature correlations with air temperature in Minnesota: Implications for climatic warming. *J. Am. Water Resour. Assoc.* **1998**, *34*, 1109–1121.
23. Ficklin, D.L.; Barnhart, B.L.; Knouft, J.H.; Stewart, I.T.; Maurer, E.P.; Letsinger, S.L.; Whittaker, G.W. Climate change and stream temperature projections in the Columbia River basin: Habitat implications of spatial variation in hydrologic drivers. *Hydrol. Earth Syst. Sci*. **2014**, *18*, 4897–4912.
24. Perez-Martin, M.A.; Estrela-Segrelles, C.; Miiiana-Albanell, C.; Mulet-Rojas, C. Water Temperature Model for Mediterranean Rivers and Climate Change, the Jucar River Case. In Proceedings of the 39th IAHR World Congress, Granada, Spain, 27 July 2022; pp. 1159–1165.
25. Wagner, I.; Izydorczyk, K.; Kiedrzyńska, E.; Mankiewicz-Boczek, J.; Jurczak, T.; Bednarek, A.; Wojtal-Frankiewicz, A.; Frankiewicz, P.; Ratajski, S.; Kaczkowski, Z.; et al. Ecohydrological system solutions to enhance ecosystem services: The Pilica River Demonstration Project. *Ecohydrol. Hydrobiol*. **2009**, *9*, 13–39.
26. Włodarczyk-Marciniak, R.; Frankiewicz, P.; Krauze, K. Socio-cultural valuation of Polish agricultural landscape components by farmers and its consequences. *J. Rural. Stud*. **2020**, *74*, 190–200.
27. Tomalski, P.; Tomaszewski, E.; Wrzesiński, D.; Sobkowiak, L. Relationships of Hydrological Seasons in Rivers and Groundwaters in Selected Catchments in Poland. *Water* **2021**, *13*, 25.
28. Błońska, D.; Grabowska, J.; Tarkan, A.S.; Soto, I.; Haubrock, P.J. Prioritising non-native fish species for management actions in three Polish rivers using the newly developed tool—Dispersal-origin-status-impact scheme. *PeerJ* **2024**, *12*, e18300. https://doi.org/10.7717/peerj.18300.
29. Jagiełło, J. *Pilica i Jej Dopływy*; Wydawnictwo CM: Warsaw, Poland, 2013; p. 123.
30. Wrzesiński, D. Flow Regime Patterns and Their Changes. In *Management of Water Resources in Poland*; Zeleňáková, M., Kubiak Wójcicka, K., Negm, A.M., Eds.; Springer Nature: Cham, Switzerland, 2021; pp. 163–180.
31. Wrzesiński, D.; Marsz, A.A.; Styszyńska, A.; Sobkowiak, L. Effect of the North Atlantic Thermohaline Circulation on Changes in Climatic Conditions and River Flow in Poland. *Water* **2019**, *11*, 1622.
32. Seland, Ø.; Bentsen, M.; Olivié, D.; Toniazzo, T.; Gjermundsen, A.; Graff, L.S.; Debernard, J.B.; Gupta, A.K.; He, Y.C.; Kirkevåg, A.; et al. Overview of the Norwegian Earth System Model (NorESM2) and key climate response of CMIP6 DECK, historical, and scenario simulations. *Geosci. Model Dev*. **2020**, *13*, 6165–6200.
33. Müller, W.A.; Jungclaus, J.H.; Mauritsen, T.; Baehr, J.; Bittner, M.; Budich, R.; Bunzel, F.; Esch, M.; Ghosh, R.; Haak, H.; et al. A higher-resolution version of the Max Planck Institute Earth System Model (MPI-ESM1.2-HR). *J. Adv. Model. Earth Syst.* **2018**, *10*, 1383–1413.
34. Döscher, R.; Acosta, M.; Alessandri, A.; Anthoni, P.; Arneth, A.; Arsouze, T.; Bergmann, T.; Bernadello, R.; Bousetta, S.; Caron, L.P.; et al. The EC-Earth3 Earth system model for the Coupled Model Intercomparison Project 6. *Geosci. Model Dev*. **2022**, *15*, 2973–3020.
35. Semmler, T.; Danilov, S.; Gierz, P.; Goessling, H.F.; Hegewald, J.; Hinrichs, C.; Koldunov, N.; Khosravi, N.; Mu, L.; Rackow, T.; et al. Simulations for CMIP6 with the AWI climate model AWI-CM-1-1. J. *Adv. Model. Earth Syst*. **2020**, *12*, e2019MS002009.
36. Xin, X.-G.; Wu, T.-W.; Zhang, J.; Zhang, F.; Li, W.-P.; Zhang, Y.-W.; Lu, Y.-X.; Fang, Y.-J.; Jie, W.-H.; Zhang, L.; et al. Introduction of BCC models and its participation in CMIP6. *Adv. Clim. Change Res*. **2019**, *15*, 533.

37. Yukimoto, S.; Kawai, H.; Koshiro, T.; Oshima, N.; Yoshida, K.; Urakawa, S.; Tsujino, H.; Deushi, M.; Tanaka, T.; Hosaka, M.; et al. The Meteorological Research Institute Earth System Model version 2.0, MRI-ESM2.0: Description and basic evaluation of the physical component. *J. Meteorol. Soc. Jpn. Ser. II* **2019**, *97*, 931–965.
38. Dunne, J.P.; Horowitz, L.W.; Adcroft, A.J.; Ginoux, P.; Held, I.M.; John, J.G.; Krasting, J.P.; Malyshev, S.; Naik, V.; Paulot, F.; et al. The GFDL Earth System Model version 4.1 (GFDL-ESM 4.1): Overall coupled model description and simulation characteristics. *J. Adv. Model. Earth Syst.* **2020**, *12*, e2019MS002015.
39. Lauritzen, P.H.; Nair, R.D.; Herrington, A.; Callaghan, P.; Goldhaber, S.; Dennis, J.; Bacmeister, J.; Eaton, B.; Zarzycki, C.; Taylor, M.A.; et al. NCAR release of CAM-SE in CESM2.0: A reformulation of the spectral element dynamical core in dry-mass vertical coordinates with comprehensive treatment of condensates and energy. *J. Adv. Model. Earth Syst.* **2018**, *10*, 1537–1570.
40. Cherchi, A.; Fogli, P.G.; Lovato, T.; Peano, D.; Iovino, D.; Gualdi, S.; Masina, S.; Scoccimarro, E.; Materia, S.; Bellucci, A.; et al. Global mean climate and main patterns of variability in the CMCC-CM2 coupled model. *J. Adv. Model. Earth Syst.* **2019**, *11*, 185– 209.
41. Jones, P.W. First-and second-order conservative remapping schemes for grids in spherical coordinates. *Mon. Weather Rev.* **1999**, *127*, 2204–2210.
42. Hoeting, J.A.; Madigan, D.; Raftery, A.E.; Volinsky, C.T. Bayesian model averaging: A tutorial (with comments by M. Clyde, David Draper and EI George, and a rejoinder by the authors. *Stat. Sci.* **1999**, *14*, 382–417.
43. Maraun, D. Bias correction, quantile mapping, and downscaling: Revisiting the inflation issue. *J. Clim.* **2013**, *2*, 2137–2143.
44. Pettitt, A.N. A non-parametric approach to the changepoint problem. *Appl. Stat*. **1979**, *28*, 126–135.
45. Kendall, M.G.; Stuart, A. *The Advanced Theory of Statistics*, 3rd ed.; Charles Griffin Ltd.: Cheshire, UK, 1968.
46. Gilbert, R.O. *Statistical Methods for Environmental Pollution Monitorin*; Van Nos-trand Reinhold Co.: New York, NY, USA, 1987.
47. Yue, S.; Pilon, P.; Phinney, B.; Cavadias, G. The influence of autocorrelation on the ability to detect trend in hydrological series. *Hydrol. Process* **2002**, *16*, 1807–1829.
48. Patakamuri, S.K.; O'Brien, N. Modified Versions of Mann Kendall and Spearman's Rho Trend Tests, Version 1.6. 31 October 2022. Available online: https://cran.r-project.org/web/packages/modifiedmk/modifiedmk.pdf (accessed on 14 September 2024).
49. Pohlert, T. Non-Parametric Trend Tests and Change-Point Detection, Version 1.1.6. 10 October 2023. Available online: https://cran.r-project.org/web/packages/trend/trend.pdf (accessed on 14 September 2024).
50. Ptak, M.; Nowak, B. Zmiany temperatury wody w Prośnie w latach 1965–2014. *Woda Sr. Obsz. Wiej.* **2017**, *17*, 101–112.
51. Rabi, A.; Hadzima-Nyarko, M.; Sperac, M. Modelling river temperature from air temperature in the River Drava (Croatia). *Hydrol. Sci. J.* **2015**, *60*, 1490–1507.
52. Durance, I.; Ormerod, S.J. Trends in water quality and discharge confound long-term warming effects on river macroinvertebrates. *Freshw. Biol.* **2009**, *54*, 388–405.
53. Ptak, M.; Heddam, S.; Haddout, S.; Sojka, M.; Amnuaylojaroen, T. Long-term changes in the thermal and ice regime of the Biebrza River (northeastern Poland) in the era of global warming. *Water* **2024**, *16*, 1–17.
54. Niedrist, G.H.; Füreder, L. Real-time warming of Alpine streams: (Re)defining invertebrates temperature preferences. *River Res.* **2021**, *37*, 283–293.
55. Grey, V.; Smith-Miles, K.; Fletcher, T.D.; Hatt, B.; Coleman, R. Empirical evidence of climate change and urbanization impacts on warming stream temperatures. *Water Res.* **2023**, *247*, 120703.
56. Liu, D.; Xu, Y.; Guo, S.; Xiong, L.; Liu, P.; Zhao, Q. Stream temperature response to climate change and water diversion activities. *Stoch. Environ. Res. Risk Assess.* **2018**, *32*, 1397–1413.
57. Morid, R.; Shimatani, Y.; Sato, T. Impact assessment of climate change on environmental flow component and water temperature—Kikuchi River. *J. Ecohydraulics* **2019**, *4*, 88–105.
58. Tang, C.; Garcia, V. Identifying stream temperature variation by coupling meteorological, hydrological, and water temperature models. *J. Am. Water Resour. Assoc.* **2023**, *59*, 665–680.
59. Hydroportal. Available online: https://wody.isok.gov.pl/imap_kzgw/?gpmap=gpPGW (accessed on 10 September 2024)).
60. Karta Charakterystyki JCWP. Pilica od Zwleczy do zb. Sulejów. Available online: https://wody.isok.gov.pl/imap_kzgw/?gpmap=gpPGW (accessed on 10 September 2024).
61. Karta Charakterystyki JCWP. Pilica od zb. Sulejów do Ujścia. Available online: https://wody.isok.gov.pl/imap_kzgw/?gpmap=gpPGW (accessed on 10 September 2024).
62. Kasushal, S.S.; Linkes, G.E.; Jaworski, N.A.; Pace, M.L.; Sides, A.M.; Seekell, D.; Belt, K.T.; Wingate, R.L. Rising stream and river temperatures in the United States. *Front. Ecol. Environ.* **2010**, *8*, 461–466.
63. Ptak, M.; Nowak, B. Variability of oxygen-thermal conditions in selected lakes in Poland. *Ecol. Chem. Eng. S* **2016**, *23*, 639–650 .
64. Zhi, W.; Ouyang, W.; Shen, C.; Li, L. Temperature outweighs light and flow as the predominant driver of dissolved oxygen in US rivers. *Nat. Water* **2023**, *1*, 1–12.
65. Penczak, T.; Kruk, A.; Zięba, G.; Marszał, L.; Koszaliński, H.; Tybulczuk, S.; Galicka, W. Ichtiofauna dorzecza Pilicy w piątej dekadzie badań. Część I. Pilica. *Rocz. Nauk. PZW* **2006**, *19*, 103–122.
66. Solovey, T. Ocena potencjalnej eutrofizacji wód płynących w zlewni środkowej Wisły. *Woda Sr. Obsz. Wiej.* **2008**, *8*, 323–336.
67. Yu, J.J.; Lee, H.J.; Lee, K.L.; Lyu, H.S.; Whang, J.W.; Shin, L.Y.; Chen, S.U. Relationship between distribution of the dominant phytoplankton species and water temperature in the Nakdong River, Korea. *Korean J. Environ. Ecol.* **2014**, *47*, 247–257.
68. Diana, A.Z.N.; Sari, L.A.; Arsad, S.; Pursetyo, K.T.; Cahyoko, Y. Monitoring of Phytoplankton Abundance and Chlorophyll-a Content in the Estuary of Banjar Kemuning River, Sidoarjo Regency, East Java. *J. Ecol. Eng*. **2021**, *22*, 29–35.

69. Tran, Y.T.H.; Pham, L.T. Relationship between water temperature and phytoplankton communities in Ba Lai River, Viet Nam. *Sci. Technol. Dev. J.* **2020**, *23*, 536–547.
70. Johnson, M.F.; Albertson, L.K.; Algar, A.C.; Dugdale, S.J.; Edwards, P.; England, J.; Gibbins, C.; Kazama, S.; Komori, D.; MacColl, A.D.C.; et al. Rising water temperature in rivers: Ecological impacts and future resilience. *Wiley Interdiscip. Rev. Water* **2024**, *11*, e1724.
71. Broadmeadow, S.B.; Jones, J.G.; Langford, T.E.L.; Shaw, P.J.; Nisbet, T.R. The influence of riparian shade on lowland stream water temperatures in southern England and their viability for brown trout. *River Res. Appl.* **2011**, *27*, 226–237.
72. Kalny, G.; Laaha, G.; Melcher, A.; Trimmel, H.; Weihs, P.; Rauch, H.P. The influence of riparian vegetation shading on water temperature during low flow conditions in a medium sized river. *Knowl. Manag. Aquat. Ecosyst.* **2017**, *418*, 5.
73. Ptak, M. Wpływ zalesienia na temperaturę wody w rzece. *Leśne Pr. Badaw.* **2017**, *78*, 251–256.